INDOOR PROPAGATION MODELING FOR RADIATING CABLE SYSTEMS IN THE FREQUENCY RANGE OF 900–2500 MHz

Jorge A. Seseña-Osorio[1, *], Alejandro Aragón-Zavala[2], Ignacio E. Zaldívar-Huerta[1], and Gerardo Castañón[3]

[1]Instituto Nacional de Astrofísica Óptica y Electrónica (INAOE), Calle Luis Enrique Erro No. 1, Tonantzintla, Puebla, C. P. 72840, México

[2]Tecnológico de Monterrey, Campus Querétaro, Epigmenio González 500, Fracc. San Pablo, Santiago de Querétaro, Querétaro, C. P. 76130, México

[3]Tecnológico de Monterrey, Campus Monterrey, Av. Eugenio Garza Sada 2501 Sur, Col. Tecnológico, Monterrey, Nuevo León, C. P. 64849, México

Abstract—The aim of this paper is to propose and evaluate a semi-empirical propagation modeling for radiating cable used in indoor environments. This propagation modeling takes into consideration propagation mechanisms such as reflections, penetration loss and cable termination that result from a particular environment, as well as specific cable paths that actual propagation models for radiating cable systems have not considered. The proposed modeling is carried out using three different propagation models and has been experimentally validated by sets of measurements performed in a university building in the frequency range from 900 MHz to 2.5 GHz. A careful selection of the data sets validates the robustness of the proposed model. The results show a mean of the error less than 1 dB while the standard deviation is between 2.2 dB and 4.6 dB in all cases. To the best of our knowledge, this is the first time such a robust modeling for radiating cable operating between 900 MHz to 2.5 GHz has been presented.

1. INTRODUCTION

Radiating cables have been extensively used recently as part of wireless systems operating in the frequency range of UHF, such as in distributed

antenna systems for in-building cellular scenarios, radio detection systems and wireless indoor positioning systems [1–4]. Because most users congregate inside buildings and stay there longer, wireless service providers are becoming more interested in delivering their services in these places. This has motivated researchers to focus their efforts on obtaining optimal coverage levels inside buildings. It is well known that for indoor wireless communications, constructive and destructive interference have a crucial effect on the signal being transmitted. Consequently, developing accurate propagation models is harder than for outdoor environments [5]. In addition, macrocell penetration at higher frequencies such as those used for UHF cellular services is too large, and although the use of repeaters may provide some coverage inside a building, capacity demands make these repeaters of limited use for more congregated buildings.

One way to distribute the signal effectively inside buildings and thus minimize multipath effects is to use distribution antenna systems [6, 7]. However there are some places such as long corridors, tunnels, airport piers, areas inside sports stadiums or underground stations in which a smooth coverage cannot easily be achieved using such systems, making radiating cable systems a good technological alternative [5, 8, 9]. A radiating cable or leaky feeder is a coaxial cable where the outer conductor has been slotted allowing radiation to occur along the cable length for uniform coverage. In the field of wireless communications, a radiating cable can be used as a passive distribution system improving coverage in any underground or closed environment [10, 11]. When used in combination with a dedicated indoor cell, such as picocell or microcell, capacity is not sacrificed and coverage can be smoothly distributed within the premises.

In terms of radio propagation modeling, some attempts have been reported with either low accuracy or impractical implementation. For instance, if a physical approach is considered, there is a model that allows the prediction of radio coverage using ray tracing [12]. The disadvantage of this approach is of the need for wall and building materials descriptions, accurate geometry and furniture/clutter, and excessive computational time for most practical design approaches. On the other hand, semi-empirical approaches to compute the radiated field of a radiating cable in indoor environments are reported by M. Liénard, et al. in [13], and K. Carter [14]. In [13], the authors describe a parametric study in the frequency domain in order to characterize the transmission channel in terms of field amplitude variation and signal fading. In order to validate this study, a straight length of radiating cable was installed in a tunnel and a series of measurements in the frequency range of 420–925 MHz were performed.

In [14], the author claims the derivation of an empirical model for the mean propagation loss for a distributed antenna system. A series of experiments were carried out in a single-story office building considering a straight length of radiating cable. In [15], the author assumes simple deployment geometries that are far from reality in the installation of such cables for practical systems. Usually, an empirical radio propagation model for a radiating cable system considers that the cable is laid as a straight line where the received power is expressed by a similar equation to that used for conventional antennas, and considering the main parameters of the radiating cable system (line loss and coupling loss), and neglecting other effects that could modify the predicted signal strength outside of the cylindrical area of influence [15, 16]. This means that in a system where the radiating cable is laid without considering different paths, the received power is evaluated with a considerable level of error.

The main goal of this paper is to establish a semi-empirical radio propagation modeling for indoor radiating cable systems in the frequency range of 900 to 2500 MHz, taking into account propagation mechanisms like reflection and penetration loss that have not yet been proposed in the literature. The development of the radio propagation modeling for radiating cables that can predict radio coverage inside buildings is very important for radio design and planning purposes. Another main difference with respect to the models previously cited is that the proposed modeling in this work considers different paths for a radiating cable, thus including other propagation mechanisms, which were previously neglected. As a consequence, the routing characteristic of a radiating cable can be used to develop different applications in internal building scenarios since this allows shaping the coverage area for more practical deployment scenarios.

In order to validate the accuracy of our proposed modeling, a series of experiments considering effects such as line loss, coupling loss, paths of radiating cable as well as the signal frequency were carried out inside a university building. Three propagation models were used and measurements were conducted at various rooms and across a corridor in which the cable was installed. The unknown parameters of the models were empirically obtained.

The paper is organized as follows: In Section 2, components of the radio propagation from radiating cables as well as the proposed modeling are described. Section 3 describes in detail the experimental setup in addition to the series of experiments carried out in order to validate the proposed modeling. Section 4 is devoted to the analysis and comparison of results. Finally, conclusions and suggestions for modeling improvements are given in Section 5.

2. PROPAGATION IN RADIATING CABLES

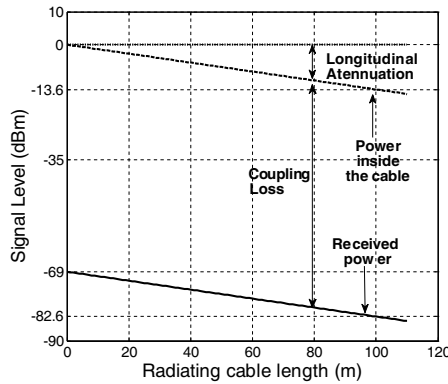### 2.1. Factors Affecting Radio Propagation from Radiating Cables

A coaxial cable acts as a radiating cable if periodic apertures are slotted in its outer conductor along the cable. These apertures allow the generation of cylindrical wave fronts that will be propagated in a radial direction outside the cable. Depending on the position of the apertures, the cables can be classified as couple-mode and radiating-mode [12]. In both cases, common characteristics for these types of cables are the so-called *longitudinal attenuation* and *coupling loss* [12]. Generally, these parameters are supplied by the manufacturer and must be taken into account at the moment of establishing a propagation model. In addition to these effects, other propagation mechanisms such as reflections and transmission must be taken into account.

2.1.1. Longitudinal Attenuation

Longitudinal attenuation is related to cable construction, conductor size and dielectric material. This parameter allows the evaluation of the signal loss in the cable and is expressed in decibels per meter [dB/m] at a specific frequency. For a given size, the value of the longitudinal attenuation increases as the frequency of operation is also increased. Table 1 shows two types of cable manufactured by RFS World, according to the producer's manual, showing this dependence. Fig. 1 illustrates the dependence of longitudinal attenuation with physical length.

Table 1. Longitudinal attenuation and coupling loss of two different cables of RFS, available in the producer's manual.

Frequency (MHz)	RCF 12-50J Size = 1/2"		RCF 78-50JA Size = 7/8"	
	Longitudinal Attenuation (dB/100 m)	Coupling Loss (dB)	Longitudinal Attenuation (dB/100 m)	Coupling Loss (dB)
450	5.70	67	3.05	75
900	8.40	66	4.4	73
1900	13.6	69	7	70
2200	14.7	70	7.8	70
2600	15.9	70	8.8	68

Figure 1. System loss that must be take into account in the planning of a radiating cable system, longitudinal attenuation $= 13.6\,\mathrm{dB}/100\,\mathrm{m}$ and coupling loss $= 69\,\mathrm{dB}$.

2.1.2. Coupling Loss

Coupling loss describes the propagation loss between the cable and a test receiver placed at a particular radial distance from the cable. In practice, coupling loss depends on several factors such as the mounting environment, cable mounting positions, the kind of mobile antenna as well as the operating frequency [12]. As for the previous case, this parameter is supplied by the manufacturer in terms of a median value, as illustrated in Table 1. Fig. 1 shows the characteristics of a RCF 12-50J cable, size $= 1/2$", having a coupling loss of $69\,\mathrm{dB}$ at $1900\,\mathrm{MHz}$, that must be taken into account for radio planning purposes.

2.1.3. Propagation Mechanisms

In a practical environment, propagation mechanisms such as reflection and diffraction due to objects, the so-called waveguiding effect, attenuation due to floor and wall penetration, etc. must be considered. As the signal propagates in space, objects with dimensions greater that the signal wavelength cause reflections. The waveguiding effect is generated when the radiating cable is near and perpendicular to corridors, thus producing multiple reflections that enhance the signal due to adding interference effects. Penetration loss should be considered when the signal travels through walls and floors made of different materials. Diffraction can be caused by sharp edges, windows and doors through which the signal travels.

The modeling of all of these effects, considering that a radiating

cable differs of a conventional antenna, requires the use of sophisticated and complex algorithms. Therefore, the goal of this work is to establish a non-complex modeling that incorporates effects such as the reflection, penetration loss and the cable termination. In Section 2.3, some of these previously mentioned effects will be illustrated.

2.2. Radiating Cable Models

The wave propagation from a radiating cable can be modeled as the radio propagation from a conventional antenna considering the transmitted power, the distance between antennas, and a particular distance considered as a reference. In this sense, the model proposed in [15] considers the main characteristics of a radiating cable system such as the longitudinal attenuation, the coupling loss and a loss factor due to blockages. Therefore, the radio propagation is determined in linear scale as:

$$P_r = \frac{P_t}{zal_cl_bd^n} \tag{1}$$

where P_r is the received power, P_t the transmitted power, za the longitudinal attenuation, l_c the coupling loss, l_b a loss factor, d the radial distance between the cable axis and the receiver, and n the loss exponent.

On the other hand, K. Carter [14] proposed a radio propagation model that considers the radiating cable as a line source and waves are spread in a cylindrical surface. A radiating cable straight section is taken into account and terminated with an antenna. In the near field and considering a mono pole antenna in the receiver, the radio propagation is modeled in linear scale as

$$P_r = P_t \frac{3\lambda^2}{8\pi^2 zadL} \tag{2}$$

where P_r is the received power, P_t the transmit power, λ the signal wavelength, za the longitudinal attenuation, d the radial distance between the cable axis and the receiver in meters, and L the radiating cable length in meters.

Finally, the Friis transmission equation is also used to validate the proposed modeling in this work. Thus considering the longitudinal attenuation, the received power in linear scale is

$$P_r = P_t \frac{\lambda^2}{(4\pi d)^2 za} \tag{3}$$

where the receive antenna and transmit antenna gains were assumed as 1. P_r is the received power, λ the signal wavelength, za the longitudinal

attenuation, and d the radial distance between the cable axis and the receiver in meters.

It is important to note that expressions (1) and (2) are valid only for the case when one straight segment of radiating cable is considered. For those cases where there is more than one straight segment or path, the use of the expressions is not reliable. On the other hand, no information is provided for cable terminations.

2.3. Proposed Radiating Cable Modeling

The modeling of all propagation mechanisms that are present in a practical indoor environment is a difficult, if not impossible, task. However, to keep the modeling simple and at the same time consider situations that have not been taken into account by other models, only the reflected rays, penetration loss, radiating cable paths and the cable termination are regarded. In particular, first reflected rays and transmission losses are calculated with empirical coefficients, which are not dependent on the wall constitutive parameters or the incident angle.

Figure 2 illustrates a radiating cable installed along a corridor. Assuming that the radiating cable generates rays that are perpendicular to cable axis, there are three paths that the signal travels. Two paths are generated due to the first reflection of the signal in walls. The distances of reflected signals in walls W1 and W2 are d_1 and d_2 respectively. Meanwhile, there is a direct ray that travels from the radiating cable to the receiver where its distance is d_0. Thus, the received
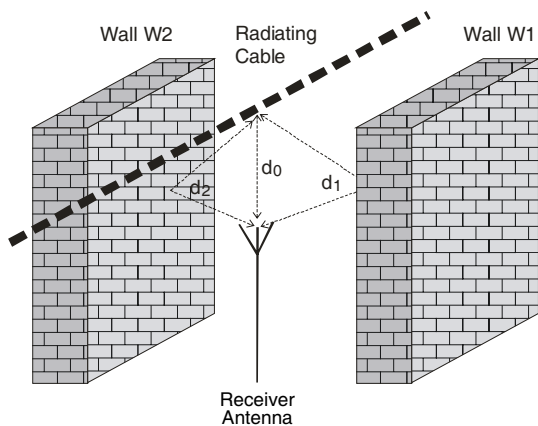
Figure 2. Multi-path generated by reflected rays and direct ray.
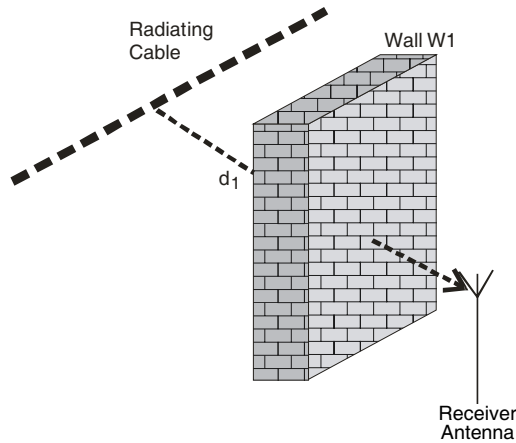
Figure 3. Transmission loss generated by wall.

power is composed by the addition of three paths and is determined as

$$P_{r\,\text{Total}} = P_r\,(d_0) + P_r\,(d_1)\,R_1 + P_r\,(d_2)\,R_2 \qquad (4)$$

where P_r can be calculated with (1), (2) or (3), and R_1 and R_2 are empirical coefficients.

Figure 3 illustrates the penetration loss generated when there is a wall between the radiating cable and the receive antenna, in this case the distance between the radiating cable and receive antenna is d_1, and the received power is

$$P_{r\,\text{Total}} = P_r\,(d_1)\,T_1 \qquad (5)$$

where P_r can be calculated with (1), (2) or (3), and T_1 is an empirical coefficient.

Figures 4 and 5 show two situations where different paths for the radiating cable are considered. Fig. 4 shows two paths or segments of radiating cable, which are close to the receiver position. Each segment generates a ray that reaches the receiver, however these rays are affected by the walls W1 and W2 (Penetration Loss). Thus the received power is

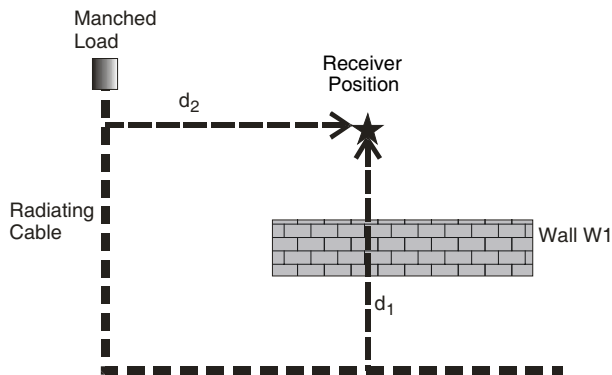$$P_{r\,\text{Total}} = P_r\,(d_1)\,T_1 + P_r\,(d_2)\,T_2 \qquad (6)$$

where P_r can be calculated with (1), (2) or (3), and T_1 and T_2 are empirical coefficients.

Finally, Fig. 5 shows a situation where there are two radiating cable segments. The received power is the sum of two rays generated by cable segments. The horizontal segment produces a ray that hits
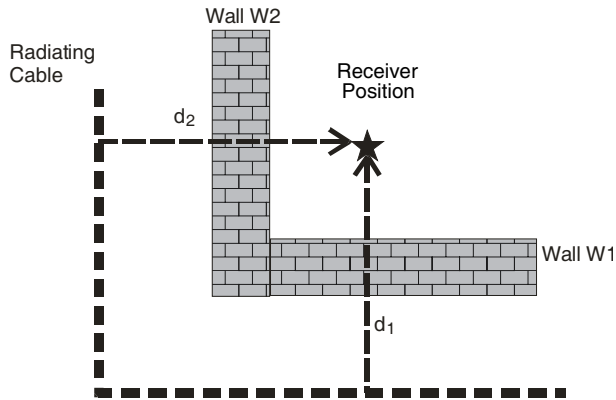
Figure 4. Two radiating cable segments that contribute to the received signal, each ray affected by penetration loss (top view).

Figure 5. Two radiating cable segments that contribute to the received signal; a ray is affected by transmission loss (top view).

the wall W1 (penetration loss), while the ray launched by the vertical segment does not find any wall. However, as special case, an empirical coefficient K is aggregated in order to incorporate the effect of the cable termination because this cable segment is terminated with a mach load. Thus the received power is

$$P_{r\,\text{Total}} = P_r\left(d_1\right)T_1 + P_r\left(d_2\right)K \qquad (7)$$

where P_r can be calculated with (1), (2) or (3), and T_1 and K are empirical coefficients.

**Figure 6.** Engineering and Electronic Centre, Building 2.

3. INDOOR RADIO MEASUREMENTS

3.1. Measurement Site

In order to validate the proposed modeling described in Section 2.3, a series of experiments were carried out in a university building that has classrooms, laboratories, offices and a warehouse. This building is a five story structure where interior and exterior walls were built with drywall and block, respectively. Ceilings were built of steel decks and metallic beams while the floors were built of ceramic tile. Ceilings are 4 meters high with false ceilings of 3 meters high. Fig. 6 shows the building. The radiating cable was placed over the false ceiling of the second level and it was laid in three paths. The first path of the radiating cable was located over the communication laboratory. The second path was positioned along the corridor and the third path placed over the warehouse. Fig. 7 shows the layout of the second level indicating the placement of the radiating cable as well as the coordinate system used in this experiment.

3.2. Measurement Equipment

RF signals were supplied by the use of a Rohde and Schwarz Signal Generator, model SMB100A, according to the producer's manual. Measurement frequencies were selected to 900, 1700, 1900, 2100, and 2500 MHz and in each case the electrical powers were 20, 20, 10, 20, and 25 dBm, respectively. The radiating cable was a RCF model 12-50J fabricated by RADIAFLEX® RFS. The use of a matched load of 50 ohms at the end of the link avoided unwanted electrical reflections. The receiver stage was composed by an omnidirectional
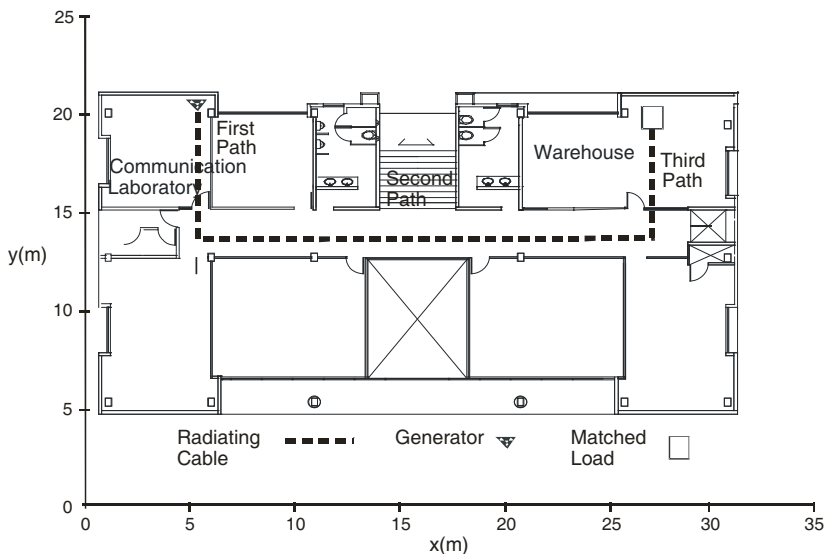
Figure 7. Layout of the second floor indicating the radiating cable position on the coordinate system.

monopole antenna plugged in to a Rohde and Schwarz Vector Network Analyzer (VNA), model ZVL6 equipped with the electrical spectrum analysis, an option that allows achieving measurements at 1700, 2100 and 2500 MHz. The experimental setup and measurement equipment used for this experiment are illustrated in Fig. 8. Also, a portable SeeGull Lx dual-band radio scanner, 900/1900 MHZ, from PCTEL, was used to achieve measurements at 900 and 1900 MHz. The software InSite v3.1.0.19 from PCTEL allows command of the scanner. In all cases the receive antenna was placed at 1.5 meters high.

3.3. Measurement Procedure

In a first step, the in-site measurement data were collected by using different trajectories (walk routes), and recorded by means of the radio scanner as well as using the spectrum analyzer option of the VNA. The walk routes were traveled at a constant speed in most of the rooms on the second level. Sample locations were recorded with the software InSite v3.1.0.19, from PCTEL, and with a special program developed in Matlab for the radio scanner and the spectrum analyzer, respectively. The entire layout of Fig. 7 was segmented in a grid of $4\lambda \times 4\lambda$ squares as illustrated in Fig. 9, where λ is the wavelength for each measurement frequency. All the samples inside
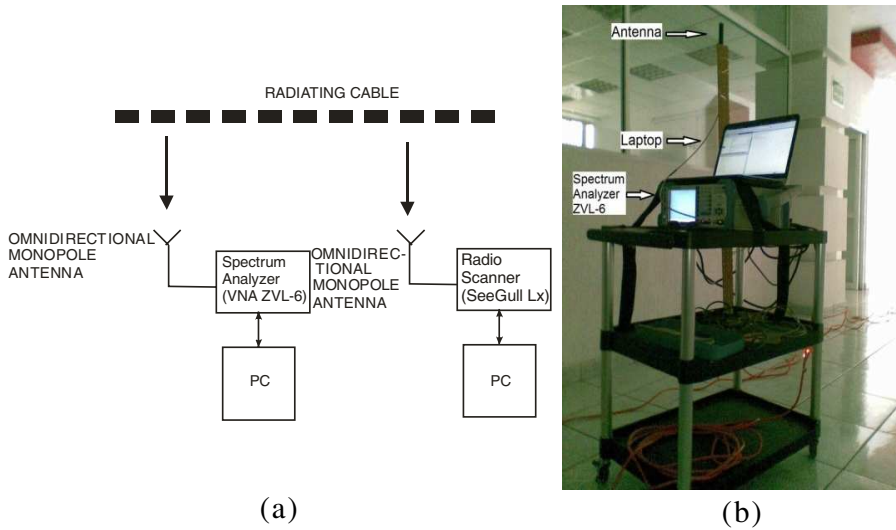
(a)   (b)

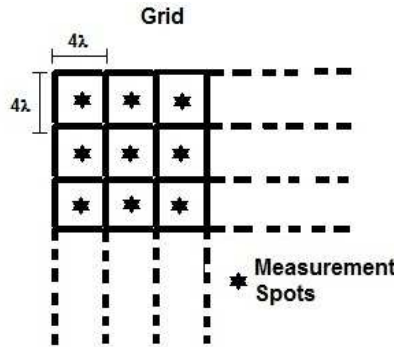**Figure 8.** Experimental setup and measurement equipment.

Figure 9. Grid used to divide the layout.

each square were averaged and represented by spots in the figure. This procedure allows recording of shadowing variations and consequently, eliminate fast-fading effects that are not required for our study [8]. Figs. 10(a) and 10(b) show experimental results corresponding to fast-fading and shadowing effects, respectively. In both cases the frequency was 1900 MHz. The fast fading was removed, averaging the samples
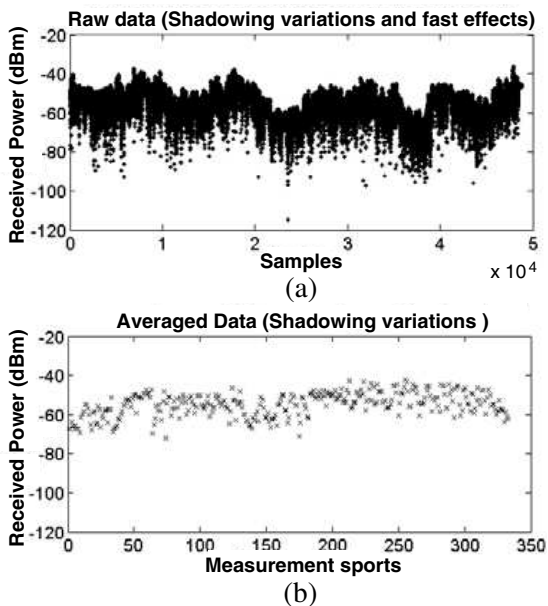
Figure 10. Fast-fading effects and shadowing variations.

by using [8].

$$\overline{P_r} = 10 \log \left(\frac{1}{n} \sum_{i=1}^{n} 10^{P_{ri}/10} \right) \tag{8}$$

where P_{ri} is the received power in dBm, and n is the number of samples inside a square of the grid.

The measurement spot set was divided into two groups, which were used for model tuning and model validation. The corresponding measurement spots for model tuning were selected for the corridor and the rooms. For the first case, measurement locations were selected everywhere along the corridor. For the second case, measurement locations were chosen considering only the corners and the middle of the rooms. Fig. 11 shows measurement locations for model tuning and model validation at 1900 MHz; for this case, 40% of measurement locations were used for model tuning. Fig. 12 illustrates measurement spots when 20% of measurement spots were used to model tuning. A similar procedure was applied to remaining frequencies. This procedure was applied in order to observe the modeling accuracy when the number of samples for model tuning is reduced. A reduced number of measurement samples allows a reduction in effort and time in the
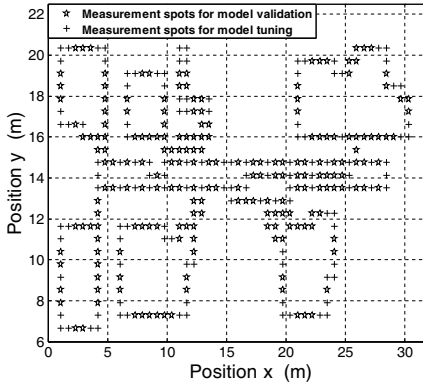
Figure 11. 40% of measurement spots used for model tuning (1900 MHz).
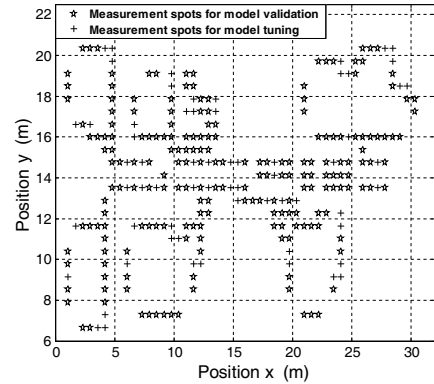
Figure 12. 20% of measurement spots used for model tuning (1900 MHz).

planning and implementation of wireless systems. On the other hand, to have confidence in the results of the experiment, most of the samples were used to model validation.

3.4. Model Calibration

An initial calibration of propagation models (Section 2.2) is necessary in order to reduce the error in the results. The environment is divided by zones. Inside each zone there are representative propagation mechanisms and nearby radiating cable paths. Fig. 13 shows the layout of the second floor with different zones that are similar to situations described in Section 2.3. The model calibration is carried out in zone 2 because there are not obstacles that could generate reflections or penetration loss, and only one cable segment is near the receiver (direct path between source and receiver).

The following procedure is applied to Equations (1), (2) and (3), but only the calibration of Equation (1) is shown. In zone 2, the main contribution in the received power is the direct ray between the radiating cable and the receiver. Thus the received power is calculated with Equation (1) and in logarithmic scale is

$$P_R = P_T - \alpha Z - L_C - L_B - 10n \log 10(d) \tag{9}$$

where P_R is the received power, P_T the transmitted power, aZ the longitudinal loss, L_C the coupling loss, d the distance between the cable and the receiver, and n the attenuation exponent which is assumed equal to 1. A calibration factor is found by the mean value
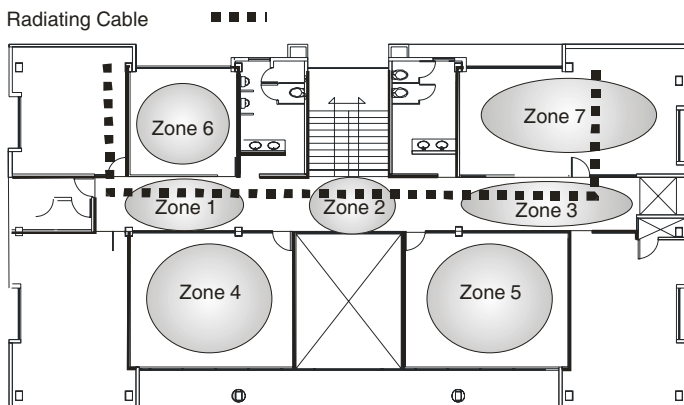
Figure 13. Second floor layout and zones to propagation modeling.

Table 2. Equations used for different environment zones.

Number of Zone	Equations in linear scale
1 and 3	$P_{r\,\text{Total Meas}} = P_{r\,\text{Theo}}(d_0) + P_{r\,\text{Theo}}(d_1)\,R_1 + P_{r\,\text{Theo}}(d_2)\,R_2$
4 and 5	$P_{r\,\text{Total Meas}} = P_{r\,\text{Theo}}(d_1)\,T_1$
6	$P_{r\,\text{Total Meas}} = P_{r\,\text{Theo}}(d_1)\,T_1 + P_{r\,\text{Theo}}(d_2)\,T_2$
7	$P_{r\,\text{Total Meas}} = P_{r\,\text{Theo}}(d_0)\,K + P_{r\,\text{Theo}}(d_1)\,T_1$

where $P_{r\text{Total Meas}}$ is the measurement received power and $P_{r\,\text{Theo}}$ the received power calculated with Equations (11), (12) or (13); d_0, d_1 and d_2 are the distances traveled by the direct ray and reflected or transmitted rays in walls. R_1, R_2, T_1, T_2 and K are empirical coefficients.

of the difference between the values calculated with (10) and the measurement values. Thus Equation (9) is

$$P_R = P_T - \alpha Z - L_C - L_B - 10n \log 10(d) + \text{CF} \qquad (10)$$

where CF is the calibration factor.

Finally the calibrated Equation (1) is

$$P_r = \frac{P_t}{z a l_c l_b d^n \text{cf}} \qquad (11)$$

where cf is the calibration factor in linear scale. Equations (12) and (13) are obtained in a similar way using (2) and (3), respectively.

In this procedure, the floor and ceiling reflections are included.

$$P_r = P_t \frac{3\lambda^2}{8\pi^2 zadL\mathrm{cf}} \tag{12}$$

$$P_r = P_t \frac{\lambda^2}{(4\pi d)^2 za\mathrm{cf}} \tag{13}$$

Table 2 shows a summary of the equations used to model the indoor radio propagation with their corresponding zones. Because the zones are similar to the situations in Section 2.3, the equations are obtained in a similar way.

To obtain reflection and transmission coefficients for the walls it is necessary to know, for example, the complex permittivity of the wall material, the wall thickness, the incident angle, polarization, etc.. At the same time, other assumptions are considered such as homogeneous walls and smooth surfaces. However this information is insufficient in multipath environments because the prediction of the signal level is not reliable. Therefore the empirical coefficients were obtained with a program. The program is run several times solving equations of Table 1 with different values of the empirical coefficients (R_1, R_2, T_1, T_2 and K), the values began from 0.01 and were increased in 0.01 steps, until a value is reached that gives a mean error near zero.

4. RESULTS

Table 3 shows the mean and standard deviation of the total error between measurement values and calculated values, which are computed with (11), (12), (13) and 40% of data set (model tuning).

Table 3. Mean and standard deviation of the total error using 40% of data set for tuning.

| Frequency (MHz)	Equation (11)		Equation (12)		Equation (13)	
	Mean error (dB)	Standard Deviation of the error (dB)	Mean error (dB)	Standard Deviation of the error (dB)	Mean error (dB)	Standard Deviation of the error (dB)
900	0.93	3.53	−0.61	3.74	0.62	4.29
1700	0.20	2.38	0.17	2.58	0.56	3.07
1900	−0.27	3.15	−0.49	2.91	0.09	3.63
2100	0.36	2.52	−0.05	2.77	0.49	2.89
2500	0.68	3.07	0.30	2.92	0.50	3.54

Table 4. Mean and standard deviation of the total error using 40% of data set for tuning.

| Frequency (MHz)	Calibrated Equation (11)		Calibrated Equation (12)		Calibrated Equation (13)	
	Mean error (dB)	Standard Deviation of the error (dB)	Mean error (dB)	Standard Deviation of the error (dB)	Mean error (dB)	Standard Deviation of the error (dB)
900	0.84	3.81	−0.38	3.94	0.87	4.64
1700	0.29	2.81	0.27	2.26	0.81	3.15
1900	−0.35	3.04	−0.35	3.38	−0.09	4
2100	0.17	2.45	−0.16	2.77	−0.39	4.09
2500	0.58	3.19	0.23	2.95	0.04	3.95
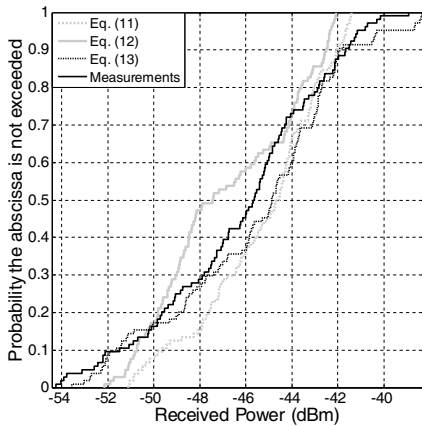
Figure 14. Cumulative distribution functions of the received power (calculated and measurement values) at 900 MHz.
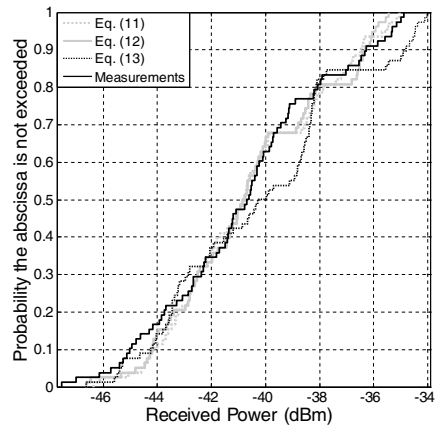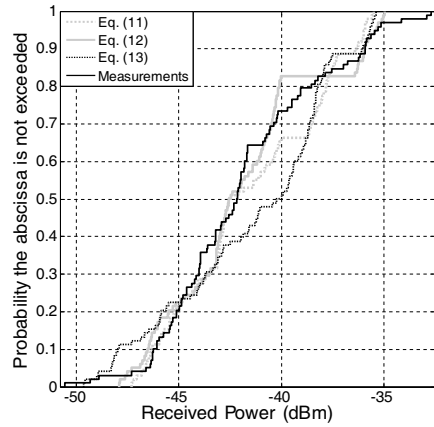
Figure 15. Cumulative distribution functions of the received power (calculated and measurement values) at 1700 MHz.

Table 4 shows the mean and standard deviation of the error between measurement values and predicted values, which are calculated with (11), (12), (13) and 20% of data set (model tuning).
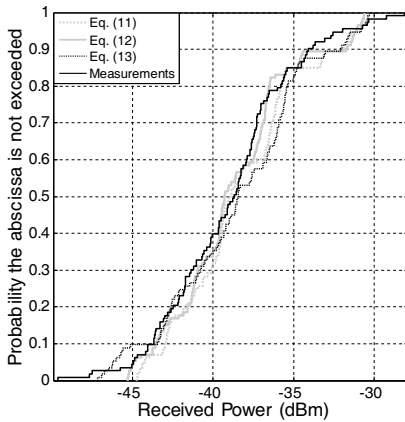
From Fig. 14 to Fig. 18, the cumulative distribution functions (CDF) of the received power are shown at all frequencies. Each
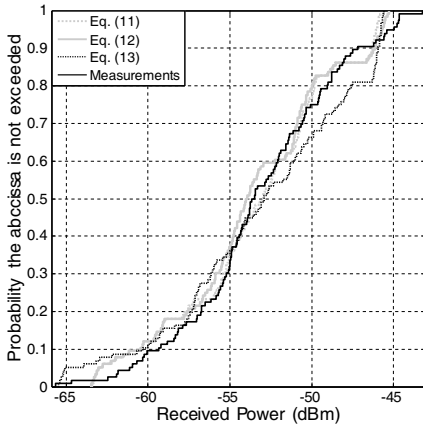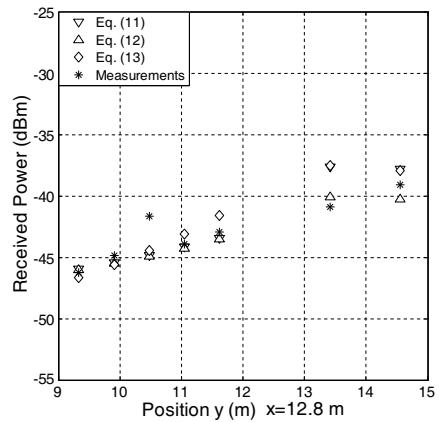
Figure 16. Cumulative distribution functions of the received power (calculated and measurement values) at 1900 MHz.

Figure 17. Cumulative distribution functions of the received power (calculated and measurement values) at 2100 MHz.
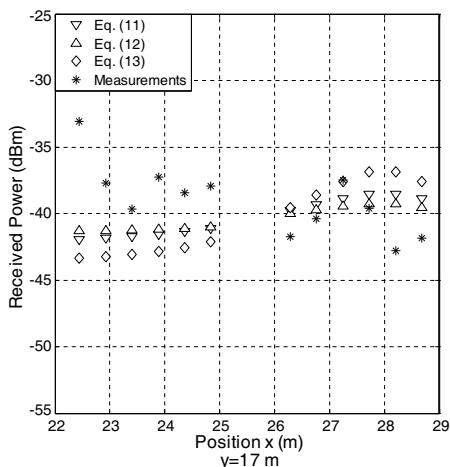

Figure 18. Cumulative distribution functions of the received power (calculated and measurement values) at 2500 MHz.

Figure 19. Received power (calculated and measurement values) along a vertical route at 2100 MHz.

graph plots the received power calculated with (11), (12) and (13). Measurement received power (CDF) is also plotted. The results of the Equation (12) show a better fit to measurements that those in Equations (11) and (13).

Figure 20. Received power (calculated and measurement values) along a horizontal route at 2500 MHz.

Figures 19 and 20 show the value of received power versus distance. These values correspond to measurements obtained along a vertical route and a horizontal route. Graphs show measured and computed values. In this last case, these values were obtained by the use of Equations (11), (12) and (13).

It is clear in Figs. 19 and 20 that computed values increase as the receiver approximates to the radiating cable. Fig. 19 corresponds to a vertical route; the received power increases when the receiver position is close to the position of the second cable segment, which is in $y = 14$ m and 5.1 m $< x < 27.8$ m. On the other hand, Fig. 20 corresponds to a horizontal route; the received power increases when the receiver position is close to the position of the third cable segment, which is in $x = 28$ m and 14 m $< y < 20$ m. These results show that the received power is influenced by the nearer cable segments and the propagation mechanisms.

5. CONCLUSIONS

A radio propagation modeling was presented for indoor radiating cable systems. The proposed modeling considers the first wall reflection, penetration loss, cable termination and radiating cable paths. The results are obtained at different frequencies. The use of different empirical coefficients allows consideration of the mentioned propagation mechanisms.

The proposed modeling was tuned and experimentally validated inside a building at frequencies of 900, 1700, 1900, 2100 and 2500 MHz. The mean and standard deviation of the error were evaluated. As was shown in the Table 3, in all cases the mean error was less than 1 dB and the standard deviation of the error is between 2.38 and 4.29 dB. In the specific case of Equation (11), results show the shortest standard deviation value of all the results (2.38 dB) at 1700 MHz. On the other hand, the results of Equation (12) show the shortest mean value of all the results (-0.05 dB) at 2100 MHz. In the case of the Equation (13), the results show the strongest standard deviation of all the results with 4.29 dB.

On the other hand, a reduction of 40% to 20% data set to tuning model was carried out, which allows the wireless system designers to decrease the time spent on carrying out the measurement campaign. Results of Table 4 show a similar behavior in the mean errors, because these are also less than 1 dB. However these are larger than those obtained with 40% of data set for tuning model and standard deviations are increased. In general terms, the results of the Equation (12) show a better fit with the measurements.

The coefficients of the proposed modeling were obtained empirically; this allows modelling different propagation mechanisms without knowing the construction material characteristics.

In summary, the proposed modeling will allow the planning of radiating cable systems in indoor environments. By means of an appropriate routing of the radiating cable inside buildings and taking into account the main propagation mechanisms, coverage areas could fulfill the requirements of the users.

Finally, the future work can be focused on the modeling of more propagation mechanisms, for instance, multiple reflections, reflections in ceiling and floor, and a detailed study of the cable termination. Also, the modeling can be tested in other environments with different characteristics in construction materials, construction configurations and routings of radiating cables.

ACKNOWLEDGMENT

REFERENCES

1. Higashino, T., K. Tsukamoto, and D. Komaki, "Radio on leaky coaxial cable (RoLCX) system and its applications," *Proceedings of PIERS*, 40–41, Beijing, China, March 2009.

2. Higashino, T., K. Tsukamoto, and D. Komaki, "Radio on LCX as universal radio platform and its application," *PIERS Proceedings*, 773–776, Xi'an, China, March 2010.

3. Nishikawa, K., T. Higashino, K. Tsukamoto, and S. Komaki, "A new position detection method using leaky coaxial cable," *IEICE Electronics Express*, Vol. 5, No. 8, 285–290, April 2008.

4. Weber, M., U. Birkel, R. Collmann, and J. Engelbrecht, "Comparison of various methods for indoor RF fingerprinting using leaky feeder cable," *Proceedings of 7th Workshop on Positioning Navigation and Communication (WPNC)*, 291–298, 2010.

5. Tolstrup, M., *Indoor Radio Planning A Practical Guide for GSM, DCS, UMTS and HSPA*, 1st Edition, Wiley, England, 2008.

6. Chen, H.-M. and M. Chen, "Capacity of the distributed antenna systems over shadowed fading channels," *Proceedings of IEEE 69th Vehicular Technology Conference*, 1–4, 2009.

7. Zhou, S., M. Zhao, X. Xu, J. Wang, and Y. Yao, "Distributed wireless communication system: A new architecture for future public wireless access," *IEEE Communications Magazine*, 108–113, March 2003.

8. Saunders, S. R. and A. Aragón-Zavala, *Antennas and Propagation for Wireless Communication Systems*, 2nd Edition, Wiley, England, 2007.

9. Stamopoulos, I., A. Aragón, and S. R. Saunders, "Performance comparison of distributed antenna and radiating cable systems for cellular indoor environments in the DCS band," *Proceedings of Twelfth International Conference on Antennas and Propagation*, 771–774, 2003.

10. Dudley, S. E. M., T. J. Quinlan, and S. D. Walker, "Ultrabroadband wireless-optical transmission links using axial slot leaky feeders and optical fiber for underground transport topologies," *IEEE Transactions on Vehicular Technology*, Vol. 57, No. 6, 3471–3476, November 2008.

11. Feng, L., X. Yang, Z. Wang, and Y. Li, "The application of leaky coaxial cable in road vehicle communication system," *Proceedings of 9th International Symposium on Antennas Propagation and EM Theory*, 1015–1018, 2010.

12. Morgan, S. P., "Prediction of indoor wireless coverage by leaky coaxial cable using ray tracing," *IEEE Transaction on Vehicular Technology*, Vol. 48, No. 6, 2005–2014, November 1999.

13. Liénard, M., P. Mariage, J. Vandamme, and P. Degauque, "Radiowave retransmission in confined areas using radiating cable: Theoretical and experimental study," *Proceedings of IEEE 44th Vehicular Technology Conference*, 938–941, 1994.

14. Carter, K., "Prediction propagation loss from leaky coaxial cable terminated with an indoor antenna," *Proceedings of 8th Virginia Tech/MPRG Symposium Wireless Communications*, 71–82, 1998.

15. Zhang, Y. P., "Indoor radiated-mode leaky feeder propagation at 2.0 GHz," *IEEE Transactions on Vehicular Technology*, Vol. 50, No. 2, 536–545, March 2001.

16. Chehri, A. and H. Mouftah, "Radio channel characterization through leaky feeder for different frequency bands," *Proceedings of IEEE 21st International Symposium on Personal Indoor and Mobile Radio Communications*, 347–351, 2010.